Suppression of absolute instability by elastic scattering in semiconductor superlattices

1997 J. Phys.: Condens. Matter 9 4853

(http://iopscience.iop.org/0953-8984/9/23/009)

J. Phys.: Condens. Matter **9** (1997) 4853–4861. Printed in the UK PII: S0953-8984(97)82171-6

Suppression of absolute instability by elastic scattering in semiconductor superlattices

X L Lei†‡ and H L Cui§

† China Centre of Advanced Science and Technology (World Laboratory), PO Box 8730, Beijing 100080, People's Republic of China

‡ State Key Laboratory of Functional Materials for Informatics, Shanghai Institute of Metallurgy, Chinese Academy of Sciences, 865 Changning Road, Shanghai, 200050, People's Republic of China

§ Department of Physics and Engineering Physics, Stevens Institute of Technology, Hoboken, NJ 07030, USA

Received 26 February 1997

Abstract. Absolute instabilities of planar semiconductor superlattices exhibiting negative differential mobility (NDM) in vertical transport are investigated using the three-dimensional hydrodynamic balance equations for arbitrary energy dispersion, with an accurate microscopic treatment of phonon and impurity scatterings. In contrast with the prediction of the drift diffusion model that in doped semiconductor superlattices absolute instability occurs closely following the onset of NDM, the present analysis shows that a planar superlattice may become absolutely unstable only when it is biased within a range deep in the NDM regime, and the enhancement of the elastic scattering suppresses the occurrence of the absolute instability. This result is in agreement with recent experimental findings, which cannot be explained within a drift diffusion model.

1. Introduction

The experimental demonstration of the Esaki–Tsu [1] negative differential mobility (NDM) and current instability in superlattice miniband transport [2–5] has brought a fascinating prospect of and encouraged intensive studies on the realization of microwave oscillators and other devices using wide-miniband semiconductor superlattices. As early as 1992, Le Person *et al* [6] reported direct observation of time-dependent current oscillation up to 20 GHz, induced by picosecond light pulses in an undoped GaAs/AlAs superlattice biased in the NDM regime and interpreted in terms of a propagating Gunn dipole domain formed by light-excited electrons having a density of the order of 3×10^{16} cm^{-3}. Recently, Grenzer *et al* [7] and Hofbeck *et al* [8] performed a series of experiments on silicon-doped GaAs/AlAs wide-miniband superlattices having a free-carrier concentration of the order of 10^{17} cm^{-3} and detected high-frequency self-sustained current oscillation and microwave radiation at a fundamental frequency of the order of 6 GHz from the superlattice over quite a large bias voltage range above the critical value (at which the DC reaches a peak). They attributed the current oscillation to propagating field domains related to the travelling space-charge-wave instability in a biased superlattice in the NDM regime.

However, as pointed out by Gueret [9], according to the drift diffusion (DD) model, in addition to the convective instability, an absolute instability may also occur in the NDM

0953-8984/97/234853+09$19.50

regime if

$$|\omega_c| > v_0^2/4D \tag{1}$$

where v_0 is the drift velocity at the bias field E_0, D is the diffusion coefficient in the DD equation and

$$\omega_c = (en_0/\epsilon_0\kappa)\mu_0 \tag{2}$$

is a frequency related to the differential mobility $\mu_0 = \partial v_0/\partial E_0$. When the absolute instability sets in, this would tend to make the device switch to a static non-uniform field distribution comprising a thin high-field layer on the anode side and a uniform low-field region in the rest of the bulk, and to destroy the condition for the formation of travelling electric-field domains [9], leading to the switch-over of the current–voltage characteristic and the disappearance of the current oscillation.

For the superlattice systems examined by Le Person *et al* [6], Grenzer *et al* [7] and Hofbeck *et al* [8] having a carrier density of the order of 10^{17} cm^{-3}, the DD model indicates (see the following text) that the systems become absolutely unstable very soon after the occurrence of the NDM. This DD-model prediction is in contradiction with the above-mentioned experimental observation that the current oscillation and microwave radiation are detected over quite a large bias-voltage range in the NDM regime. To gain physical insight into this problem it is desirable to pursue further analyses of the absolute instability in superlattice miniband transport beyond the DD model.

The purpose of this paper is to carry out a careful examination on the absolute instability in a doped semiconductor superlattice, using the non-parabolic balance-equation method [10, 11] extended to spatially non-uniform systems [10, 12]. This method, which is fully three dimensional in nature and takes microscopic scattering mechanisms into account, not only is much more sophisticated than the DD model but also should be more accurate than the previous one-dimensional calculations [13, 14], especially for systems with a high carrier density. We find that, in contrast with the DD-model prediction, the balance-equation analysis shows that a doped planar superlattice may become absolutely unstable only when it is biased within a finite range deep in the NDM regime, and the enhancement of the elastic scattering suppresses the occurrence of the absolute instability. This result is in agreement with recent experimental findings which cannot be explained by the DD model.

2. Hydrodynamic balance equations for superlattices

In the non-parabolic hydrodynamic balance-equation method [10] the transport state of a system consisting of many electrons moving in an arbitrary energy band, which are subject to an applied electric field and scattered by impurities and by phonons, is described by the shifted lattice momentum $\boldsymbol{p}_d$, the electron temperature T_e, and the chemical potential μ (or the ratio of the chemical potential to the electron temperature, $\zeta \equiv \mu/T_e$). These fundamental variables are treated as time and space dependent and all the other quantities are functions of these fundamental variables. Requiring balances of the carrier number density, the acceleration and the energy in a small volume element about a spatial position, we obtain the the hydrodynamic balance equations as given in [10].

Consider a planar superlattice in which electrons move freely in the transverse (x–y) plane and can travel along the growth axis (z direction) through the (lowest) miniband formed by the periodic potential wells and barriers of finite height. The electron energy dispersion consists of a transverse energy $\varepsilon_{\boldsymbol{k}_\parallel} = k_\parallel^2/2m$ (m being the band mass of the

carrier in the bulk semiconductor), and a tight-binding miniband energy $\varepsilon(k_z)$ related to the longitudinal motion:

$$\varepsilon(\boldsymbol{k}) = \varepsilon_{\boldsymbol{k}_\parallel} + \varepsilon(k_z) \tag{3}$$

with

$$\varepsilon(k_z) = (\Delta/2)[1 - \cos(k_z d)] \tag{4}$$

Here, $\boldsymbol{k} = (\boldsymbol{k}_\parallel, k_z)$ where $\boldsymbol{k}_\parallel = (k_x, k_y)$ and k_z are the in-plane and longitudinal wavevectors ($-\infty < k_x, k_y < \infty$, and $-\pi/d < k_z \leqslant \pi/d$, d being the superlattice period along the z-direction) and Δ is the miniband width.

When an electric field E is applied along the superlattice growth axis, the carrier drift motion, the frictional acceleration and the spatial inhomogeneity are all in the z direction. The hydrodynamic balance equations take the form

$$\frac{\partial n}{\partial t} = -\frac{\partial}{\partial z}(n v_d) \tag{5}$$

$$\frac{\partial}{\partial t}(n v_d) = -\frac{\partial}{\partial z}(n B_z) + \frac{neE}{m_z^*} + nA \tag{6}$$

$$\frac{\partial}{\partial t}(n\epsilon) = -\frac{\partial}{\partial z}(n S_z) + neE v_d - nW. \tag{7}$$

Here, the carrier density n, the drift velocity v_d, the average per-carrier energy ϵ, the zz component $1/m_z^*$, of the inverse effective-mass tensor, the zz component B_z of the average velocity–velocity dyadic, the z component S_z of the energy flux vector, the frictional acceleration A due to impurity and phonon scatterings and the carrier energy-loss rate W to the lattice system are all functions of $z_d \equiv p_d d$, T_e and ζ. Their expressions were given in [10]. The Poisson equation is written as

$$\frac{\partial E}{\partial z} = \frac{e}{\epsilon_0 \kappa}(n - n_0) \tag{8}$$

where κ is the dielectric constant of the bulk material and n_0 is the background density of positive charge which is assumed to be uniformly distributed over the whole superlattice.

3. Dispersion relation for small wave-like fluctuations

To investigate the occurrence of instability in the biased condition in superlattice miniband transport, we consider a small wave-like fluctuation superimposed on a DC bias quantity, writing z_d, T_e, ζ, E and any other physical quantity Q involved in equations (5)–(8) as the sum of the DC bias part and a small fluctuation: $z_d = z_0 + \delta z_d$, $T_e = T_0 + \delta T_e$, $\zeta = \zeta_0 + \delta\zeta$, $E = E_0 + \delta E$ and $Q = Q_0 + \delta Q$ (Q stands for v_d, n, $1/m_z^*$, B_z, S_z or ϵ), with δz_d, δT_e, $\delta\zeta$, δE and $\delta Q \sim \exp[\mathrm{i}(kz - \omega t)]$.

The equations for the bias DC quantities are just those for DC steady-state transport in the spatially homogeneous case and were discussed in detail in [11]. The main result is that v_0 as a function of E_0 exhibits NDM; after reaching its peak value v_p at $E_0 = E_c$, v_0 decreases with increasing E_0.

For linear order of small fluctuations the equations can be written in terms of δz_d, δT_e, $\delta\zeta$ and δE. The Poisson equation (8) and the continuity equation (5) become

$$\frac{en_0}{\epsilon_0 \kappa}(\alpha_{0t}\,\delta T_e + \alpha_{0\zeta}\,\delta\zeta) - \mathrm{i}k\,\delta E = 0 \tag{9}$$

and

$$(kv_m\alpha_{10}\cos z_0)\,\delta z_d + (kv_m\alpha_{1t}\sin z_0 - \omega\alpha_{0t})\,\delta T_e + (kv_m\alpha_{1\zeta}\sin z_0 - \omega\alpha_{0\zeta})\,\delta\zeta = 0. \tag{10}$$

Equations (6) and (7) are

$$c_{31}\,\delta z_d + c_{32}\,\delta T_e + c_{33}\,\delta\zeta + c_{34}\,\delta E/E_0 = 0 \tag{11}$$

$$c_{41}\,\delta z_d + c_{42}\,\delta T_e + c_{43}\,\delta\zeta + c_{44}\,\delta E/E_0 = 0. \tag{12}$$

Here, c_{3j} and c_{4j} $(j = 1, 2, 3)$, which depend on the DC bias and scattering, are functions of k and ω:

$$c_{31} \equiv -\frac{1}{v_m}\frac{\partial A_0}{\partial z_d} + \omega_B\alpha_{10}\sin z_0 + \mathrm{i}kv_m\alpha_{20}\sin(2z_0) - \mathrm{i}\omega\alpha_{10}\cos z_0$$

$$c_{32} \equiv -\frac{1}{v_m}\frac{\partial A_0}{\partial T_e} - \omega_B\alpha_{1t}\cos z_0 + \mathrm{i}kv_m\tfrac{1}{2}[\alpha_{0t} - \alpha_{2t}\cos(2z_0)] - \mathrm{i}\omega\alpha_{1t}\sin z_0$$

$$c_{33} \equiv -\frac{1}{v_m}\frac{\partial A_0}{\partial \zeta} - \omega_B\alpha_{1\zeta}\cos z_0 + \mathrm{i}kv_m\tfrac{1}{2}[\alpha_{0\zeta} - \alpha_{2\zeta}\cos(2z_0)] - \mathrm{i}\omega\alpha_{1\zeta}\sin z_0$$

$$c_{34} \equiv -\omega_B\alpha_{10}\cos z_0$$

and

$$c_{41} \equiv \frac{2}{\Delta}\frac{\partial W_0}{\partial z_d} - \omega_B\alpha_{10}\cos z_0 + \mathrm{i}kv_m[\alpha_{10}\cos z_0 - \alpha_{20}\cos(2z_0) + \beta_{10}\cos z_0] - \mathrm{i}\omega\alpha_{10}\sin z_0$$

$$c_{42} \equiv \frac{2}{\Delta}\frac{\partial W_0}{\partial T_e} - \omega_B\alpha_{1t}\sin z_0 + \mathrm{i}kv_m\left(\alpha_{1t}\sin z_0 - \frac{\alpha_{2t}}{2}\sin(2z_0) + \beta_{1t}\sin z_0\right) + \mathrm{i}\omega(\alpha_{1t}\cos z_0 - \alpha_{0t} - \beta_{0t})$$

$$c_{43} \equiv \frac{2}{\Delta}\frac{\partial W_0}{\partial \zeta} - \omega_B\alpha_{1\zeta}\sin z_0 + \mathrm{i}kv_m\left(\alpha_{1\zeta}\sin z_0 - \frac{\alpha_{2\zeta}}{2}\sin(2z_0) + \beta_{1\zeta}\sin z_0\right) + \mathrm{i}\omega(\alpha_{1\zeta}\cos z_0 - \alpha_{0\zeta} - \beta_{0\zeta})$$

$$c_{44} \equiv -\omega_B\alpha_{10}\sin z_0.$$

In these equations, $\omega_B = edE_0$ is the Bloch frequency at the bias field E_0, $\alpha_{i0} \equiv \alpha_i(T_0, \zeta_0)$ $(i = 1, 2)$, $\beta_{i0} \equiv \beta_i(T_0, \zeta_0)$ $(i = 0, 1)$, $\alpha_{it} \equiv \partial\alpha_i(T_0, \zeta_0)/\partial T_e$ $(i = 0, 1, 2)$, $\alpha_{i\zeta} \equiv \partial\alpha_i(T_0, \zeta_0)/\partial\zeta$ $(i = 0, 1, 2)$, $\beta_{it} \equiv \partial\beta_i(T_0, \zeta_0)/\partial T_e$ $(i = 0, 1)$, and $\beta_{i\zeta} \equiv \partial\beta_i(T_0, \zeta_0)/\partial\zeta$ $(i = 0, 1)$. The functions $\alpha_i(T_0, \zeta_0)$ $(i = 0, 1, 2)$ and $\beta_i(T_0, \zeta_0)$ $(i = 0, 1)$ were defined in [12].

Equations (9)–(12) constitute a set of four linear algebraic equations for four variables δz_d, δT_e, $\delta\zeta$ and δE. The condition for it to have non-zero solution requires that the determinant of its coefficients vanishes:

$$D(k, \omega) = 0. \tag{13}$$

Equation (13) is the dispersion equation which has been used to analyse travelling space-charge-wave modes in GaAs-based superlattices [12]. It was found that superlattice systems exhibit convective instability when it is biased in the NDM regime. Although the predicted phase velocity and amplitude growth rate of the convective space-charge waves differ greatly from the previous understanding of the DD model, the observation that amplitude-growing travelling space-charge waves occur as long as $E_0 > E_c$, is in agreement with the DD model.

4. Absolute instability

Generally, the dispersion equation (13) maps a point of the complex frequency (ω) plane onto a point or several points of the complex wavevector (k) plane. The possible absolute instability of an infinite superlattice system may be analysed by the behaviour of such a mapping [9]. It is known that an absolute instability occurs if there is a value of ω having a positive imaginary part, at which two roots of the dispersion equation, which correspond to waves travelling in different directions, coincide [15].

As an example we perform a systematic analysis at lattice temperature $T = 300$ K for a GaAs-based superlattice with period $d = 4.8$ nm, miniband width $\Delta = 660$ K and carrier sheet density $N_s = 0.48 \times 10^{15}$ m^{-2}. The carrier bulk density of this system is $n = N_s/d = 1.0 \times 10^{17}$ cm^{-3}. We consider electron scattering by acoustic and polar optical phonons having bulk-like modes of GaAs, as well as the elastic scattering due to charged impurities. The strength of the latter is assumed so that the low-temperature linear DC mobility of the system is $\mu_0 = 2.0$ m^2 V^{-1} s^{-1}. The DC steady-state drift velocity v_0 as a function of the electric field E_0 obtained from the zero-order balance equations exhibits behaviour typical of negative differential conductance when the bias electric field E_0 is larger than the threshold field $E_c \simeq 5.6$ kV cm^{-1}.

Figure 1 demonstrates a mapping determined from the dispersion equation (13) by showing several lines (labelled 1, 2 and 3 respectively) of the ω plane mapped onto the k plane in the case of DC bias $E_0 = 8.0$ kV cm^{-1}. Line 1 ($\omega_1/2\pi = 50$ GHz) of the ω plane is mapped into two curves in the k plane labelled 1; line 2 ($\omega_1/2\pi = -50$ GHz) of the ω plane is mapped into curves labelled 2 in the k plane. When ω moves downwards along the imaginary axis (line 3) of the ω plane towards the point $\omega = \mathrm{i}\omega_b$ ($\omega_b/2\pi = -25.7$ GHz), the two drift relaxation solutions in the k plane move along the imaginary axis, from positive and negative sides, respectively, towards the position $k = \mathrm{i}k_b$ ($k_b d = -0.156$). When ω, in its descent along the imaginary axis, passes through $\mathrm{i}\omega_b$, the corresponding drift relaxation solutions start from $\mathrm{i}k_b$ and go almost horizontally in opposite directions. Therefore, the position $\omega_1 = 0$, $\omega_2 = \omega_b$ and $k_1 = 0$, $k_2 = k_b$ is apparently a double root of equation (13). This double root corresponds to an absolute instability if ω_b is positive [9]. Although for the case shown in figure 1 ($E_0 = 8.0$ kV cm^{-1}) ω_b is negative, it value increases with increasing strength of the bias electric field and becomes positive from $E_0 = 9.2$ kV cm^{-1} to $E_0 = 14.1$ kV cm^{-1}. In this bias range the space–time dependence of the system response is essentially proportional to

$$\exp(\omega_b t - k_b z)$$

indicating temporal growth without spatial propagation. The calculated ω_b- and k_b-values of the double root for different bias electric fields are shown in figure 2. Despite the fact that, when the bias electric field E_0 enters the NDM regime ($\mu_0 < 0$), the system immediately exhibits convective instability, this superlattice becomes absolutely unstable only when the bias field E_0 exceeds 9.2 kV cm^{-1}, in favour of temporal growth of the local domain. The domain size can be estimated from the value of k_b to be several spatial periods of the superlattice. Thus, for a realistic superlattice having more than several tens of spatial periods, the condition for the onset and formation of such local domains should not be seriously affected by the boundary conditions. When an absolute instability sets in, any anode-type non-uniformity can nucleate a local growing high-field domain and thus would tend to make the device switch to a non-uniform field distribution comprising a thin stationary high-field layer on the anode side and a uniform low-field region in the rest of the bulk [9].

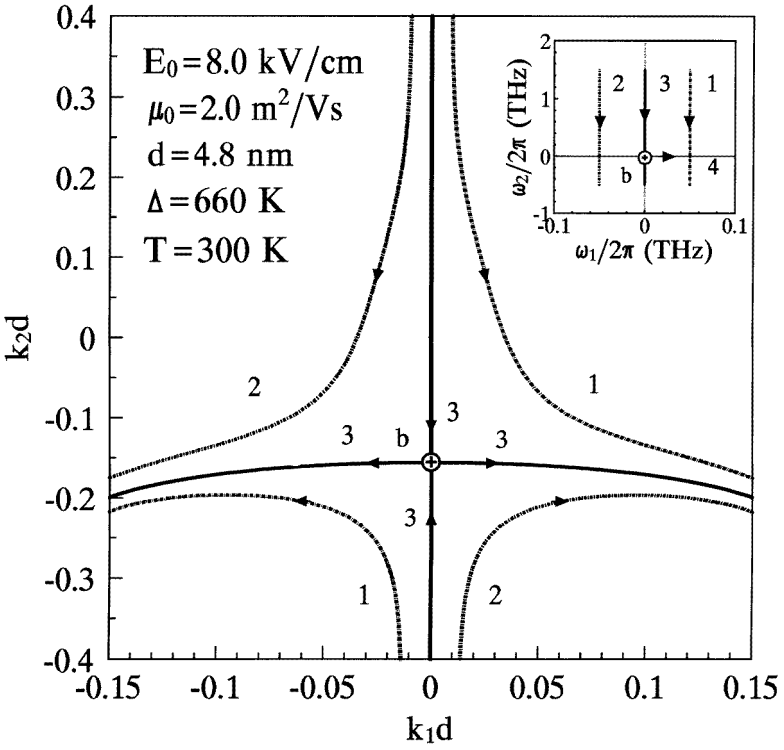

Figure 1. Mapping of the ω plane onto the k plane for a GaAs-based superlattice having a period $d = 4.8$ nm, a miniband width $\Delta = 660$ K, a carrier sheet density $N_s = 0.48 \times 10^{15}$ m^{-2} and a low-temperature linear DC mobility $\mu_0 = 2.0$ m^2 V^{-1} s^{-1} at a bias field $E_0 = 8.0$ kV cm^{-1}. The lattice temperature is $T = 300$ K. Each line (labelled 1, 2 and 3) in the ω plane is mapped into two curves in the k plane. The double root at $k_1 = 0$, $k_2 = k_b$ ($k_b d = -0.156$) corresponds to $\omega_1 = 0$, $\omega_2 = \mathrm{i}\omega_b$. For the bias case illustrated here ($E_0 = 8.0$ kV cm^{-1} and $\omega_b/2\pi = -25.7$ GHz) there is no absolute instability.

Such a condition for the occurrence of absolute instability in a doped semiconductor superlattice is quite different from the condition (1) set by the conventional DD model. For the superlattice specified above, the diffusion coefficient can be estimated from $D = \Delta^2 d^2 \tau/8$ with the momentum relaxation time $\tau \simeq 0.12$ ps [16]. Since v_0 is always less than the peak drift velocity $v_p \simeq 53.9$ km s^{-1}, we have $v_0^2/4D < 2.8 \times 10^{11}$ s^{-1}. ω_c can be obtained from the v_0 versus E_0 (see figure 2). It is seen that, for this system, the condition (1) is satisfied within a very large range of bias fields E_0 from 5.8 to about 100 kV cm^{-1}. Therefore, according to the criterion (1) of the DD model, this superlattice will be absolutely unstable almost immediately following the occurrence of the NDM.

5. Comparison with experiments

Recently, Grenzer *et al* [7] and Hofbeck *et al* [8] detected high-frequency self-sustained current oscillations and microwave radiation in several silicon-doped GaAs/AlAs wide-miniband superlattices having a free-carrier concentration of the order of 10^{17} cm^{-3} and attributed the current oscillation to propagating field domains related to the travelling

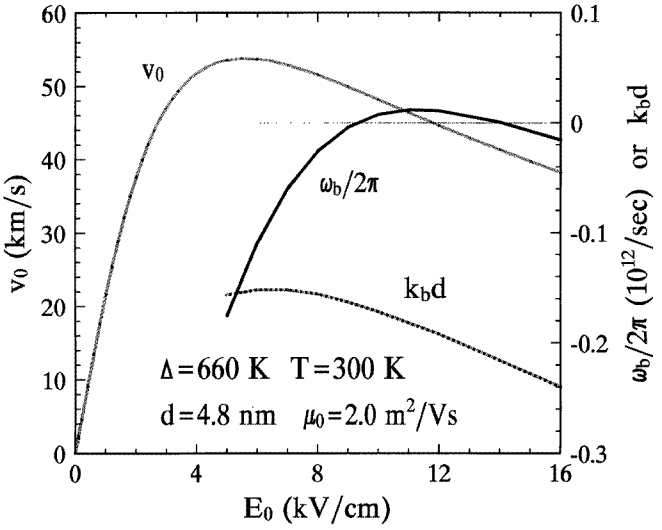

Figure 2. Values of ω_b and $k_b d$ of the double root shown as functions of the bias field E_0 for the same GaAs-based superlattice as described in figure 1 at a lattice temperature $T = 300$ K. The drift velocity v_0 is also shown here (shaded curve).

space-charge-wave instability. One of their systems examined consists of 120 periods, each having 13 monolayers (3.68 nm) of GaAs and four monolayers (1.12 nm) of AlAs. Using the Kronig–Penny model we estimate that the width of the lowest miniband is about $\Delta \simeq 57$ meV (660 K). This essentially has the same miniband structure as the sample superlattice that we discussed in the preceding section except that the electrons should suffer stronger elastic scattering (owing to impurities, surface roughness, etc). To mimic the experimental system with a threshold field $E_c \simeq 10$ kV cm^{-1}, we assume that the low-temperature linear DC mobility $\mu_0 = 0.1$ m^2 V^{-1} s^{-1}. This yields the curve of v_0 versus E_0 (obtained from the zero-order balance equations) shown in figure 3, having a threshold field $E_c \simeq 10.2$ kV cm^{-1}. From this curve of v_0 versus E_0 and using the method illustrated in the preceding section to estimate, we find that the criterion (1) will be satisfied when the bias field $E_0 > 10.5$ kV cm^{-1} up to $E_0 = 65$ kV cm^{-1}.

We can also make an estimation from the simplified balance-equation model [16]. Based on this simplified model the condition (1) can be written approximately as

$$\frac{E_0}{E_c} - 1 > 2\alpha(T)\frac{\epsilon_0 \kappa E_c^2}{n_0 \Delta} \tag{14}$$

where $\alpha(T)$ is a function depending on Δ/T and roughly of the order of 0.4 for $\Delta = 57$ meV at room temperature. Therefore, for the above-mentioned GaAs-based superlattices used in the experiments, condition (1) would be satisfied if $E_0/E_c - 1 > 0.04$, or $E_0 > 10.6$ kV cm^{-1}.

This means that, according to criterion (1), the DD model still predicts the system to become absolutely unstable very soon after it enters the NDM regime or when the bias voltage goes above U_c. The onset of the absolute instability would switch the superlattice from the propagating field-domain state to the spatially stationary non-uniform field distribution state, having essentially no current oscillation in the system. The observation of the current oscillations indicates that such a prediction is not correct, and

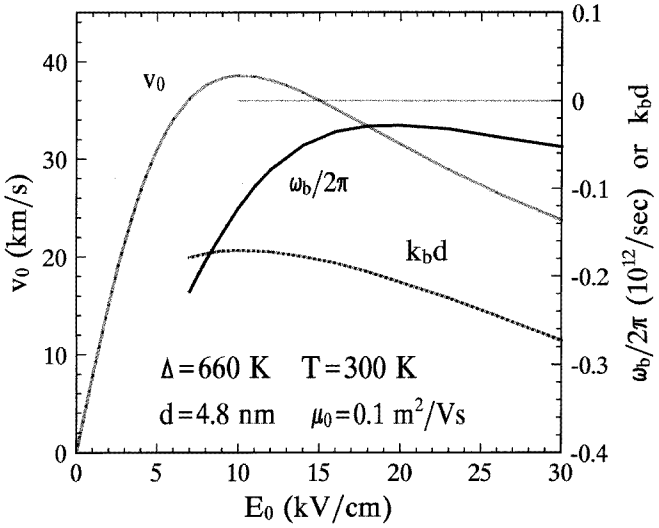

Figure 3. Values of ω_b and $k_b d$ of the double root, shown as functions of the bias field E_0 at a lattice temperature $T = 300$ K for the GaAs-based superlattice with the same miniband structure and carrier density as described in figure 1 but having a low-temperature linear DC mobility $\mu_0 = 0.1$ m^2 V^{-1} s^{-1}. The drift velocity v_0 is shown (shaded curve).

the absolute instability does not occur at least over a substantial part of the NDM regime in this system.

To compare the present balance-equation model with experiments, we have repeated the mapping analysis as outlined in the preceding section for the GaAs-based superlattice with exactly the same miniband structure and carrier density as described in figures 1 and 2, but having stronger elastic scattering as outlined above (with low-temperature linear DC mobility $\mu_0 = 0.1$ m^2 V^{-1} s^{-1} and threshold field $E_c = 10.2$ kV cm^{-1}). The calculated ω_b- and k_b-values of the double root as functions of the bias electric field are shown in figure 3. We see that ω_b is always negative, i.e. the absolute instability does not occur in this system. Such a result confirms that within the whole NDM regime this superlattice favours a propagating field-domain state, in agreement with the experimental observation.

6. Conclusion

We have investigated the possible absolute instability in doped wide-miniband GaAs-based planar superlattices at room temperature, using the three-dimensional hydrodynamic balance equations recently developed for an arbitrary energy band. We considered carriers scattered by both the acoustic and the polar optical phonons in GaAs as well as by impurities (to mimic the elastic scattering). In contrast with the prediction of the DD model that in doped semiconductor superlattices absolute instability occurs closely following the onset of NDM, we find that, although a planar superlattice with weak elastic scattering may become absolutely unstable when it is biased within a range deep in the NDM regime, the enhancement of the elastic scattering would completely suppress the occurrence of the absolute instability. This result is in agreement with recent experimental findings, which cannot be explained within a DD model.

Acknowledgments

The authors thank the National Natural Science Foundation of China, the China National and Shanghai Municipal Commissions of Science and Technology, the Shanghai Foundation for Research and Development of Applied Materials, and the Army Research Office of the US (contract No DAAH04-94-G-0413) for support of this work.

References

[1] Esaki L and Tsu R 1970 *IBM J. Res. Dev.* **14** 61
[2] Sibille A, Palmier J F, Wang H and Mollot F 1990 *Phys. Rev. Lett.* **64** 52
[3] Beltram F, Capasso F, Sivco D L, Hutchinson A L and Chu S N G 1990 *Phys. Rev. Lett.* **64** 3167
[4] Grahn H T, von Klitzing K, Ploog K and Döhler G H 1991 *Phys. Rev.* B **43** 12 094
[5] Hadjazi M, Sibille A, Palmier P J and Mollot F 1992 *Electron. Lett.* **27** 1101
[6] Le Person H, Minot C, Boni L, Palmier J F and Mollot F 1992 *Appl. Phys. Lett.* **60** 2397
[7] Grenzer J *et al* 1995 *Ann. Phys., Lpz.* **4** 184
Grenzer J *et al* 1996 *Proc. 23nd Int. Conf. on the Physics of Semiconductors (Berlin 21–26 July 1996)* ed M Scheffler and R Zimmermann p 1663
[8] Hofbeck K *et al* 1996 *Phys. Lett.* **218A** 349
[9] Gueret P 1971 *Phys. Rev. Lett.* **27** 256
[10] Lei X L 1992 *Phys. Status Solidi.* b **170** 519
Lei X L 1995 *Phys. Status Solidi.* b **190** K1
[11] Lei X L, Horing N J M and Cui H L 1991 *Phys. Rev. Lett.* **66** 3277
Lei X L, Horing N J M and Cui H L 1992 *J. Phys.: Condens. Matter* **4** 9375
[12] Lei X L, Horing N J M and Cui H L 1995 *J. Phys.: Condens. Matter* **7** 9811
[13] Büttiker M and Thomas H 1977 *Phys. Rev. Lett.* **38** 78
Büttiker M and Thomas H 1978 *Solid-State Electron.* **21** 95
[14] Ignatov A A and Shashkin V I 1987 *Sov. Phys.–JETP* **66** 526
[15] Bonch-Bruevich V L, Zvyagin I P and Mironov A G 1975 *Domain Electric Instabilities in Semiconductors* (New York: Consultant Bureau) ch 3
[16] Lei X L, Horing N J M and Cui H L 1993 *Superlatt. Microstruct.* **14** 243
Lei X L, Horing N J M and Cui H L 1994 *Appl. Phys. Lett.* **65** 2984